Journal of
Biomedical Optics

SPIEDigitalLibrary.org/jbo

Qualitative near-infrared vascular imaging system with tuned aperture computed tomography

Tatsuhiko Matsushita
Tosiaki Miyati
Kazuya Nakayama
Takashi Hamaguchi
Yoshihiko Hayakawa
Allan G. Farman
Shigeki Ohtake

SPIE

Journal of Biomedical Optics 16(7), 076004 (July 2011)

Qualitative near-infrared vascular imaging system with tuned aperture computed tomography

Tatsuhiko Matsushita,[a,b] Tosiaki Miyati,[a,b] Kazuya Nakayama,[a] Takashi Hamaguchi,[a,c] Yoshihiko Hayakawa,[d] Allan G. Farman,[e] and Shigeki Ohtake[a,b]
[a]Kanazawa University, Graduate School of Medical Science, Division of Health Science, 5-11-80 Kodatsuno, Kanazawa, 920-0942, Japan
[b]Kanazawa University, Institute of Medical, Pharmaceutical and Health Science, Wellness Promotion Science Center, 5-11-80 Kodatsuno, Kanazawa, 920-0942, Japan
[c]Kanazawa University Hospital, Department of Radiology, 13-1 Takara-machi, Kanazawa, 920-8641, Japan
[d]Kitami Institute of Technology, Department of Computer Science, Faculty of Engineering, 165 Koen-cho, Kitami, Hokkaido, 090-8507, Japan
[e]University of Louisville School of Dentistry, Division of Radiology and Imaging Science, Department of Surgical and Hospital Dentistry, Louisville, Kentucky 40292

Abstract. We developed a novel system for imaging and qualitatively analyzing the surface vessels using near-infrared (NIR) radiation using tuned aperture computed tomography (TACT®). The system consisted of a NIR-sensitive CCD camera surrounded by sixty light emitting diodes (with wavelengths alternating between 700 or 810 nm). This system produced thin NIR tomograms, under 0.5 mm in slice thickness. The venous oxygenation index reflecting oxygen saturation levels calculated from NIR tomograms was more sensitive than that from the NIR images. This novel system makes it possible to noninvasively obtain NIR tomograms and accurately analyze changes in oxygen saturation. [DOI: 10.1117/1.3595424]

Keywords: near infrared; tuned aperture computed tomography; near infrared tomogram; venous oxygenation index.

Paper 10642PR received Dec. 8, 2010; revised manuscript received Apr. 6, 2011; accepted for publication May 9, 2011; published online Jul. 8, 2011.

1 Introduction

The regional vascular oxygenation level provides very important clinical information for the analysis of biological conditions. Vascular oxygenation levels need to be measured as an aid to monitor blood oxygen levels and saturation; therefore, noninvasive measurement methods under realistic biological conditions have been developed.[1–5] These are permitted by measurement method using near infrared (NIR). Systems described in the literature are based on a specific characteristic that NIR is absorbed by the hemoglobin in blood.[6] Additionally, development of noncontact sensing methods to define the location of the near surface veins holds considerable promise for aiding in obtaining blood samples from individuals whose veins are not evident from visual inspection.[7] Such capability would be especially useful for infants and those with elevated BMI values. Since NIR can transmit through thin regions such as through a finger, vascular images can be easily acquired[8,9] and monitoring blood oxygen saturation can be easily measured.[10] Although using a transmission method is limited to thin regions, this study developed a novel system for the noninvasive imaging of surface vessels in thick regions where NIR imaging is not always feasible. Additionally, NIR tomograms using tuned aperture computed tomography (TACT®) were obtained, as well as measurements of the regional vascular oxygenation levels.

In this paper, we demonstrated the utility of this system and described its characteristics and potential future in clinical applications.

2 Materials and Methods

2.1 *System*

A NIR-sensitive charged-coupled device (CCD) camera (XC-EI50/50CE, Sony Corporation, Tokyo, Japan) was surrounded by sixty light emitting diodes (LED) (alternating wavelengths between 700 to 810 nm, VSF706C1 and LSF811C1, Optrans, Tokyo, Japan), that could only detect NIR from subcutaneous tissues (Fig. 1). The NIR was absorbed across surface vessels more than any other surrounding tissues.

2.2 *Tuned Aperture Computed Tomography Theory*

TACT is a reconstruction method that can be used to synthesize three-dimensional representation from multiple arbitrary prerecorded two-dimensional basis images (each acquired at a different angle) of an interesting region. The basic principles of the TACT algorithm are derived from the optical aperture theory and tomosynthesis.[11,12] The TACT stacks the basis images, inputs locations of fiducial markers for each basis image, and reconstructs a series of arbitrary multiplanner cross-sectional images. Stability for maintaining continuity in geometric is required for the generation of three-dimensional images, such as computed tomography, at the time of collection of images. However, TACT enables an arbitrary setup of projection directions,

Address all correspondence to: Tatsuhiko Matsushita, Kanazawa University, Graduate School of Medical Science, Division of Health Science, 5-11-80 Kodatsuno, Kanazawa, 920-0942, Japan; Tel: 81-76-2652500; Fax: 81-76-2344351; E-mail: tmatusi@mhs.mp.kanazawa-u.ac.jp.

1083-3668/2011/16(7)/076004/5/$25.00

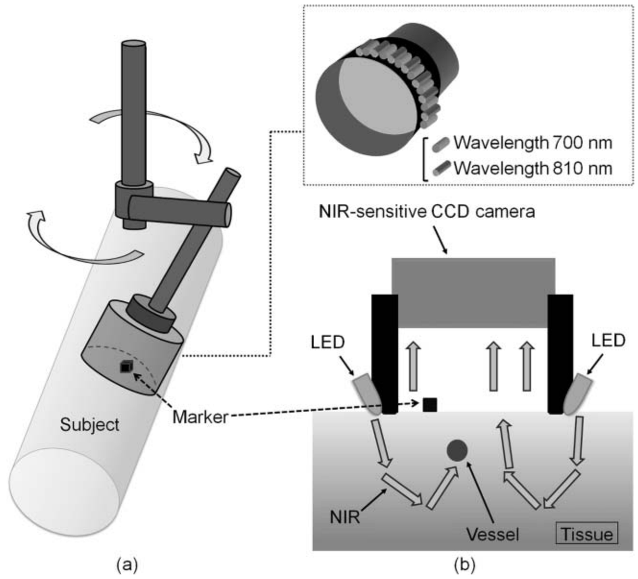

Fig. 1 (a) Acquisition system and (b) schematic diagram for NIR imaging.

because the position of the fiducial markers is always available. Moreover, because image reconstruction often involves only shifting and adding two-dimensional images, the process is rapidly and efficiently managed by even the simplest image-processing computers. Iterative restoration is often utilized in TACT imaging in an attempt to improve detailed clarity.[13,14] The iterative restoration algorithm works for the deblurring of TACT slices to remove out-of-focus noise. TACT has been used in the clinical application of digital mammography[15] and oral surgery using x-ray emitting devices,[16] whereas there has been no study, that we are aware of, that reconstructed NIR tomograms.

2.3 *Tomograms*

To increase the image contrast of the vessels and obtain three-dimensional information, we created tomograms calculated from NIR images (basis images) using the TACT program (TACT Workbench version 0.9.43). First, for the TACT series, a fiducial marker was used by attaching approximately 1 mm wire to the forearm skin within the field of view. Next, when considering the factors influencing the image accuracy of TACT,[17–19] six concentric NIR projections of surface vessels including the marker were obtained and reconstructed as tomograms (Fig. 2). The angular disparity was set at 30 deg during each projection. Reconstructed images were processed by using the proprietary iterative restoration algorithm three times (default setting).

2.4 *Venous Oxygenation Index*

Multiple NIR images (six projections in total) of surface vessels on the forearm were obtained before and after the loading test, that is, using a blood pressure cuff on the upper arm at each wavelength in accordance with the optical aperture theory[11,12] during the first second. We held the cuff pressure at more than 140 mmHg to occlude vessels. Then, tomograms were created using the TACT program and the venous oxygenation index (VOI) was calculated from the image signal intensities at each wavelength [Eq. (1)], which is an indicator of the oxygen

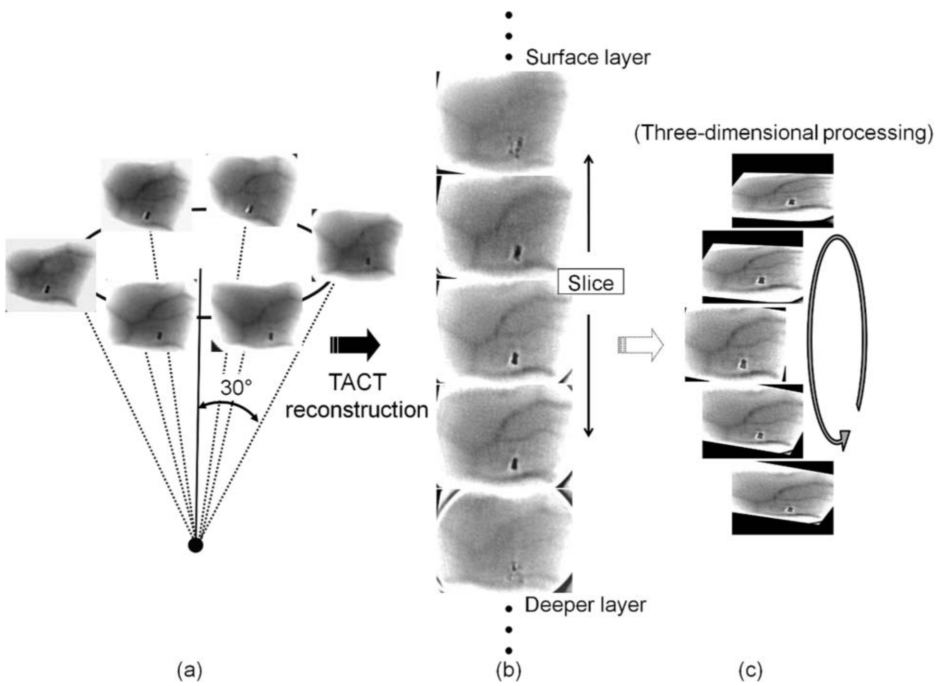

Fig. 2 One example for TACT procedure. (a) NIR images (wavelengths: 810 nm) of surface vessels and projection geometry relationships between angular disparity and numbers of projections performed. (b) TACT slices reconstructed from (a). (c) Rotated three-dimensional data structures from (b).

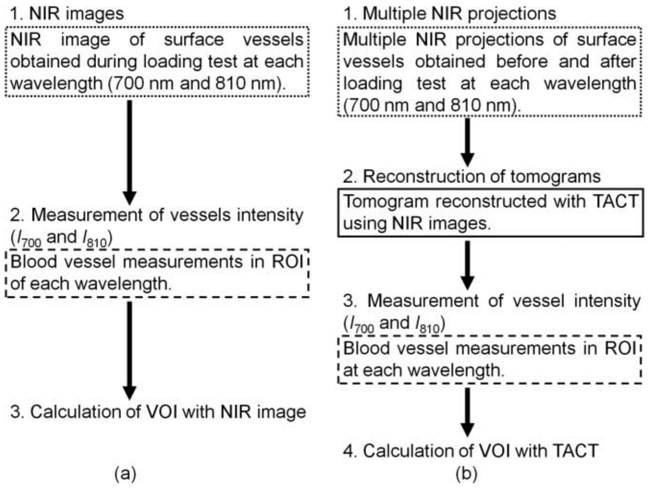

Fig. 3 VOI measurement procedures (a) without and (b) with tomograms.

saturation level,[20]

$$VOI = \frac{I_{700}}{I_{810}}, \tag{1}$$

where I_{700} and I_{810} are the signal intensities of the vessels for the 700 and 810 nm images, respectively. Figure 3 shows the measurement procedure for the calculation of VOI. Moreover, the VOI was compared to the oxygen saturation (SpO_2) using a pulse oximeter. The study was performed in five healthy volunteers after informed consent was obtained from each human subject.

2.5 *System Characteristics*

Correlation between the current supplied to the LED and the signal intensity of the NIR images was investigated, because signal intensity of a NIR image is relative value. When the current to the LED at each wavelength, respectively, was slowly increased to the maximum value, NIR images of LED light were obtained by CCD camera and the signal intensities of these images were measured.

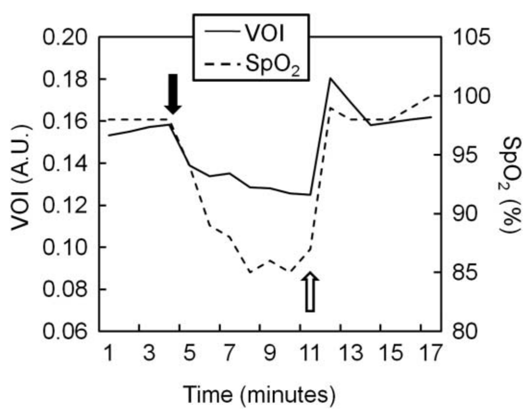

Fig. 4 Change in venous oxygenation index and SpO_2 during the loading test. Black arrow shows cuff pressure on and white arrow shows cuff pressure off. Note that there was good agreement with VOI and SpO_2. A.U.: arbitrary unit.

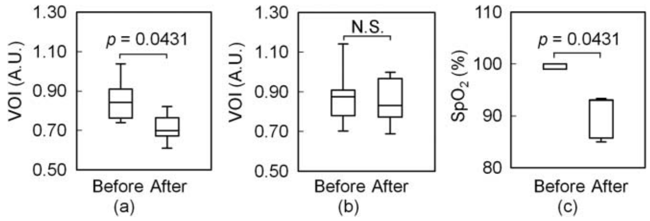

Fig. 5 Change in VOI (a) with and (b) without TACT, and (c) change in oxygen saturation (SpO_2) measured by pulse oximeter before and after loading test. VOI with TACT and SpO_2 after loading test were significantly greater than before. However, there was no significant difference in VOI without TACT (P value = 0.345). A.U.: arbitrary unit; N.S.: not significant.

In addition, we evaluated the effective slice-thickness of our system using a chart, which is a specially designed apparatus for the measurement of tomographic slice-thickness. This chart was placed at an angle $11^\circ 32'$ relative to the tomographic plane. Six concentric projections of chart images were obtained and reconstructed as a tomogram using the TACT program. Slice-thickness property was visually evaluated by one of the authors.

2.6 *Statistical Methods*

The Wilcoxon signed-rank test was used to assess differences in VOI and SpO_2 before and after a loading test. Multiple linear regression analysis was used to assess the relation between the current supplied to the LED and the signal intensity of the NIR images.

3 Results

Our system was capable of acquiring several projections for the tomograms within a few seconds in thick regions that cannot transmit [Fig. 2(a)] and easily reconstructs a tomogram using the TACT program [Fig. 2(b)].

VOI was good correlated with SpO_2 in this system during the loading test using a blood pressure cuff (Fig. 4). Both VOI with TACT and SpO_2 after the loading test were significantly lower than those before the loading test (P value = 0.0431, P value = 0.0431), but VOI without TACT showed no significant difference (P value = 0.345 (Fig. 5).

There was a high correlation between the signal intensity of NIR images and the current supplied to the LED at each wavelength in Fig. 6 ($R^2 = 0.998$, P value < 0.001 in 700 nm, $R^2 = 0.999$, P value < 0.001 in 810 nm). The effective slice-thickness of our system was 0.4 mm [Fig. 7(b)].

4 Discussion

A transmitted beam is generally used for NIR imaging,[8,9] but this system would obtain NIR images in thick regions that cannot transmit [Fig. 2(a)]. Some methods to obtain tomograms using NIR are reported,[21,22] but require lengthy imaging times, in the order of more than ten minutes, with the additional restraint of limited scan regions. We could obtain several projections for the tomograms within a few seconds and easily reconstruct a tomogram using TACT and even three-dimensional images [Figs. 2(b) and 2(c)]. TACT is usually used in an x-ray system

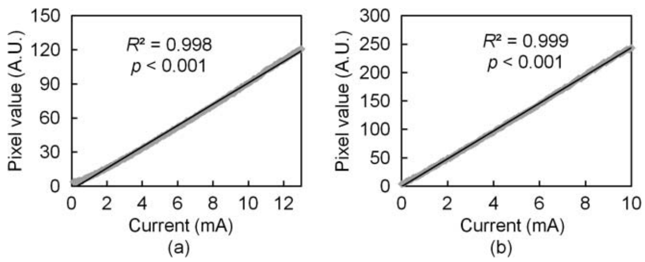

Fig. 6 Relationship between the signal intensity of NIR images and current (mA) in (a) 700 and (b) 810 nm LED. There was a high correlation between the signal intensity of NIR images and the current supplied to the LED at each wavelength. A.U.: arbitrary unit.

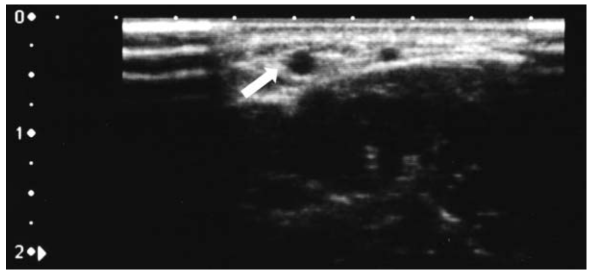

Fig. 8 Forearm surface vessels image by ultrasound. White arrow shows median antebrachial vein, which is 2.0 mm in diameter. Surface to vein distance is 5.0 mm.

(radiography is used as a basis image).[11–19] Although there has been no study that reconstructed NIR tomograms, the TACT reconstruction process in our system was a similar method to that in the x-ray system. Therefore, the number of projections needed to reconstruct the tomography, the accuracy of the method, and robustness of the method are not different between the x-ray system and our system.

VOI and SpO_2 demonstrated good correlation in this system (Fig. 4). The result indicates that we can evaluate oxygen saturation of surface vessels. After the cuff pressure was released, the VOI temporarily tended to rise compared to before the loading test. It is assumed that the blood flow volume temporarily increased as the blood flow was interrupted by the load and was rapidly effused when the cuff pressure was released. Moreover, measurement sensitivity was improved when tomograms were used for the calculation of VOI (Fig. 5), because tomograms can only evaluate the blood signals. However, the NIR image signal without TACT overlapped with the surrounding thick tissue signal. Although, at least six NIR images were required to reconstruct the tomograms, all images were acquired within one second. Thereby, temporary resolution is satisfied with the loading test for evaluating the oxygenation change. We used a pulse oximeter as the gold standard to measure SpO_2 and compared these findings with VOI, since it was desired to exclusively use noninvasive methods.

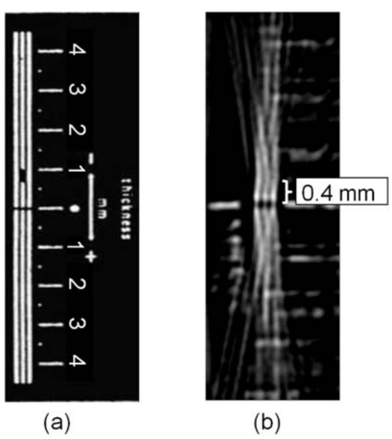

Fig. 7 (a) Picture of chart and (b) NIR image for assessing the slice thickness of NIR with TACT. Scale corresponding to the slice-thickness of the tomogram.

To analyze VOI, it is necessary that the relationship between NIR radiation and signal intensities of the images is linear, because signal intensity of an NIR image is relative value. In this study, there was a linear dependency between the current supplied to the LED and the image signal intensity (Fig. 6). Because it is already known that the relationship between the NIR signal intensity and current supplied to LED is linear,[23,24] linearity between NIR radiation and image signal intensities was verified by this study in the range where VOI was measured. Therefore, we can independently measure VOI of image signal intensity.

In tomosynthesis, slice-thickness is considered to be in relation to the angular disparity of the projection geometry, as in tomography. The effective slice-thickness of our system was 0.4 mm [Fig. 7(b)]. This was considered appropriate because forearm blood vessels used for the calculation of VOI were 2 mm in diameter (Fig. 8).

However, it must be noted that there are some variables in the measurement of VOI. First, the distance between the skin and CCD camera could have an impact on the acquired image data, because the focus of the lens mounted CCD camera of this system was matched to the surface vessels. Thus, NIR repeated scattering in air could be detected by the CCD camera, which might contribute to a decrease in image contrast. In the next series of studies, a grid will be attached, which is an optical fiber bundle, between the skin and CCD camera to decrease scattering effects. The different path lengths of the NIR transmitting subcutaneous tissue might cause different signal intensity attenuations. Therefore, an attenuation correction method by the analysis of skin tissues spatial fluorescence distribution by Monte Carlo simulation is required.[25,26] Additionally, to increase measurement precision of VOI, we need to establish a correction method of image inhomogeneous sensitivity at each wavelength.

We cannot show the advantage compared to the previous method on relevant NIR imaging, but it could enhance the proposed method, because, theoretically, the summation of images increases signal-to-noise ratio and image contrast of vessels compared with a single NIR image. Moreover, the ability to acquire three-dimensional spatial information would increase the diagnostically useful information available over that of a conventional two-dimensional display. Indeed, measurement sensitivity was improved when tomograms were used for the calculation of VOI. Of course, further clinically relevant investigations should be pursued in the future.

In future clinical works, we would like to apply our system to evaluate Reynaud's syndrome and torsion of the testis decreasing the regional vascular, tissue viability of skin grafts and bedsores, as well as skin inflammation due to breast radiation therapy.

5 Conclusion

This novel imaging system makes it possible to noninvasively obtain NIR tomograms containing three-dimensional information that can then be used to accurately analyze changes in oxygen saturation levels. There are several clinical applications for which this system will be best utilized, such as to increase treatment efficacy or to detect early symptoms of the adverse effects of radiation on the sensitive tissues of the skin. Further clinical studies are required to refine the system for everyday clinical usage.

References

1. M. Siegemund, J. Bommel, and C. Ince, "Assessment of regional tissue oxygenation," *Intensive Care Med.* **25**(10), 1044–1060 (1999).
2. S. Suzuki, S. Takasaki, T. Ozaki, and Y. Kobayashi, "A tissue oxygenation monitor using NIR spatially resolved spectroscopy," *Proc. SPIE* **3597**, 582–592 (1999).
3. D. A. Boas, T. Gaudette, G. Strangman, X. Cheng, J. J. Marota, and J. B. Mandeville, "The accuracy of near infrared spectroscopy and imaging during focal changes in cerebral hemodynamics," *Neuroimage* **13**(1), 76–90 (2001).
4. Y. Yoshitake, H. Ue, M. Miyazaki, and T. Moritani, "Assessment of lower-back muscle fatigue using electromyography, mechanomyography, and near-infrared spectroscopy," *Eur. J. Appl. Physiol.* **84**(3), 174–179 (2001).
5. A. Lima and J. Bakker, "Noninvasive monitoring of peripheral perfusion,"*Intensive Care Med.* **31**(10), 1316–1326 (2005).
6. W. A. Eaton, L. K. Hanson, P. J. Stephens, J. C. Sutherland, and J. B. R. Dunn, "Optical spectra of oxy- and deoxyhemoglobin," *J. Am. Chem. Soc.* **100**, 4991–5003 (1978).
7. H. D. Zeman, G. Lovhoiden, and C. Vrancken, "The clinical evaluation of vein contrast enhancement," in *Proc. 26th Ann. Int. Conf. IEEE Engineering in Medicine and Biology Society*, pp. 1203–1206 (2004).
8. M. Kono, H. Ueki, and S. Umemura, "Near-infrared finger vein patterns for personal identification," *Appl. Opt.* **41**(35), 7429–7436 (2002).
9. N. Miura, A. Nagasaka, and T. Miyatake, "Feature extraction of finger-vein patterns based on repeated line tracking and its application to personal identification," *Mach. Vision Appl.* **15**(4), 194–203 (2004).
10. S. J. Fearnley, "Pulse oximetry," *Update in Anaesthesia, Practical Procedures* **5**(2), 1 (1995).
11. R. L. Webber, R. A. Horton, D. A. Tyndall, and J. B. Ludlow, "Tuned-aperture computed tomography (TACT$^{\mathrm{TM}}$). Theory and application for three-dimensional dento-alveolar imaging," *Dentomaxillofac Radiol.* **26**(1), 53–62 (1997).
12. R. L. Webber and W. Bettermann, "A method for correcting for errors produced by variable magnification in three-dimensional tuned aperture computed tomography," *Dentomaxillofac Radiol.* **28**(5), 305–310 (1999).
13. M. Abreu, Jr., D. A. Tyndall, J. B. Ludlow, and C. J. Nortjé, "The effect of the number of iterative restorations on tuned aperture computed tomography for approximal caries detection," *Dentomaxillofac Radiol.* **30**(1), 325–329 (2001).
14. M. K. Nair, H. G. Gröndahl, R. L. Webber, U. P. Nair, and J. A. Wallace, "Effect of iterative restoration on the detection of artificially induced vertical radicular fractures by tuned aperture computed tomography," *Oral Surg. Oral Med. Oral Pathol. Oral Radiol. Endod.* **96**(1), 118–125 (2003).
15. R. L. Webber, H. R. Underhill, and R. I. Freimanis, "A controlled evaluation of tuned-aperture computed tomography applied to digital spot mammography," *J. Digit Imaging* **13**(2), 90–97 (2000).
16. K. Yamamoto, Y. Hayakawa, Y. Kousuge, M. Wakoh, H. Sekiguchi, M. Yakushiji, and A. G. Farman, "Diagnostic value of tuned-aperture computed tomography versus conventional dentoalveolar imaging in assessment of impacted teeth," *Oral Surg. Oral Med. Oral Pathol. Oral Radiol. Endod.* **95**(1), 109–118 (2003).
17. K. Yamamoto, A. G. Farman, R. L. Webber, R. A. Horton, and K. Kuroyanagi, "Effects of projection geometry and number of projections on accuracy of depth discrimination with tuned-aperture computed tomography in dentistry," *Oral Surg. Oral Med. Oral Pathol. Oral Radiol. Endod.* **86**(1), 126–130 (1998).
18. K. Yamamoto, K. Nishikawa, N. Kobayashi, K. Kuroyanagi, and A. G. Farman, "Evaluation of tuned aperture computed tomography depth discrimination for image series acquired variously with linear horizontal, linear vertical and conical beam projection arrays," *Oral Surg. Oral Med. Oral Pathol. Oral Radiol. Endod.* **89**(6), 766–770 (2000).
19. A. G. Farman, J. P. Scheetz, P. D. Eleazer, M. J. Edge, L. Gettleman, R. D. Morant, S. Limrachtamorn, and K. Yamamoto, "Tuned-aperture computed tomography accuracy in tomosynthetic assessment for dental procedures," *International Congress Series* **126**, 695–699 (2001).
20. T. Ozawa, T. Saito, S. Numada, T. Nishiyasu, and N. Kondou, "Measurement of venous oxygen pressure by non invasive blood vessel monitor 'ASTRIM'," *Trans. Jpn. Soc. Med. Biol. Eng.* **40** (Suppl), 178 (2002).
21. D. M. Richter, "Computed tomography laser mammography, a practical review," *Nippon Igaku Hoshasen Gakkai Zasshi* **59**(6), 687–693 (2003).
22. X. Wang, D. L. Chamberland, P. L. Carson, J. B. Fowlkers, R. O. Bude, D. A. Jamadar, and B. J. Roessler, "Imaging of joints with laser-based photoacoustic tomography: an animal study," *Med. Phys.* **33**(8), 2691–2697 (2006).
23. Optrans, available at http://www.optrans.com/pdf/220-LSF811C1.PDF, Accessed 7 December (2010).
24. Optrans, available at http://www.optrans.com/pdf/217-VSF706C1.PDF, Accessed 7 December (2010).
25. D. Y. Churmakov, I. V. Meglinski, S. A. Piletsky, and D. A. Greenhalgh, "Analysis of skin tissues spatial fluorescence distribution by the Monte Carlo simulation," *J. Phys. D: Appl. Phys.* **36**, 1722–1728 (2003).
26. I. V. Meglinski and S. J. Matcher, "Computer simulation of the skin reflectance spectra," *Comput. Methods Programs Biomed.* **70**(2), 179–186 (2003).